

TILTROTOR MODELLING FOR SIMULATION IN VARIOUS FLIGHT CONDITIONS

MAREK MILLER

Institute of Aviation, Warsaw
e-mail: m.miller@ilot.edu.pl

JANUSZ NARKIEWICZ

Institute of Aeronautics and Applied Mechanics, Warsaw University of Technology
e-mail: jnark@meil.pw.edu.pl

A computer model of a tilt-rotor has been developed for calculating performance, simulating flight and investigating stability and control. The model is composed of a fuselage, wings, an empennage, engine nacelles and rotors. Tiltrotor equations of motion have been obtained by summing up inertia, gravity and aerodynamic loads acting on each part of the aircraft. Aerodynamic loads at wings, empennage and rotor blades have been calculated using a quasisteady model. For rotor induced velocity, the Glauert model has been used. The influence of the rotor inflow wing and empennage aerodynamic loads has been found using the actual value of induced velocity. The computer program of tilt-rotor model has been developed in the MatLab environment. The sub-programs for load calculation have been supplemented by modules for calculation of trim states and stability and control matrices. During the first stage of model investigation, steady flight conditions were calculated, which gave insight into rotorcraft behaviour and model quality.

Key words: tiltrotor, rotorcraft, flight control, simulation

Notations

Indicies

| | | |
|-----|---|---|
| a | – | aerodynamic |
| b | – | inertia |
| c | – | related to three-dimensional body (fuselage, nacelle) |
| f | – | fuselage |

| | |
|---------------|--|
| g, G | – gravity |
| h | – horizontal stabilizer |
| i | – inertia |
| $I = 1$ | – element (wing, nacelle, rotor) on right side of aircraft |
| $I = 2$ | – element (wing, nacelle, rotor) on left side of aircraft |
| $J = 1, 2, 3$ | – rotor blade index of i -th rotor |
| m | – aerodynamic moment, moving element, mass |
| n | – nacelle |
| p | – aircraft, fuselage |
| r | – rotor |

Matrices and vectors

| | |
|--------------------------|---|
| \mathbf{A} | – rotation matrix of moving element, $\mathbf{A} = \mathbf{A}(\phi, \varphi, \gamma)$ |
| \mathbf{A}_G | – aircraft rotation matrix |
| \mathbf{A}_r | – transformation matrix of coordinate system in airfoil |
| \mathbf{A}_V | – velocity matrix |
| \mathbf{C} | – control vector, $\mathbf{C} = [\tau, \delta_w, \delta_h, \delta_v, \Theta]^\top$ |
| \mathbf{I}_x | – inertia matrix of x -th element |
| $k_{()}$ | – coefficients of inflow due rotors and wings |
| \mathbf{Q}_{xy} | – y -th loads of x -th element, $\mathbf{Q}_{xy} = [\mathbf{F}_{xy}, \mathbf{M}_{xy}]^\top$ |
| \mathbf{V} | – vector of linear velocity in $O_p x_p y_p z_p$, $\mathbf{V} = [U, V, W]^\top$ |
| \mathbf{V}_a | – section velocity |
| \mathbf{V}_c | – vector of linear velocity of three-dimensional body |
| \mathbf{U} | – induced velocity in $O_p x_p y_p z_p$ |
| \mathbf{W} | – wind velocity in $O_p x_p y_p z_p$ |
| $\Delta \mathbf{W}_{()}$ | – inflow due rotors and wings in $O_p x_p y_p z_p$ |
| \mathbf{X} | – vector of aircraft motion, $\mathbf{X} = [\mathbf{V}, \boldsymbol{\Omega}, \mathbf{x}_g, \boldsymbol{\Phi}]^\top = [U, V, W, P, Q, R, x_g, y_g, z_g, \Phi, \Theta, \Psi]^\top$ |
| \mathbf{Y}_x | – state vector of x -th element |
| \mathbf{g} | – vector of gravity acceleration |
| \mathbf{g}_p | – vector of gravity acceleration in $O_p x_p y_p z_p$ |
| \mathbf{r}_{CG} | – position of C.G. in $O_p x_p y_p z_p$ |
| \mathbf{r}_{nCG} | – position of C.G. in moving element coordinate system |
| \mathbf{r}_n | – position of moving element coordinate system in $O_p x_p y_p z_p$ |
| \mathbf{x}_g | – translation of aircraft relative to ground, $\mathbf{x}_g = [x_g, y_g, z_g]^\top$ |
| $\boldsymbol{\Omega}$ | – vector of angular velocity in $O_p x_p y_p z_p$, $\boldsymbol{\Omega} = [P, Q, R]^\top$ |
| $\boldsymbol{\Omega}_p$ | – velocity matrix of plane (non-moving element) |
| $\boldsymbol{\Omega}_m$ | – velocity matrix of moving element |
| $\boldsymbol{\Phi}$ | – Euler's angles described as vector, $\boldsymbol{\Phi} = [\Phi, \Theta, \Psi]^\top$ |
| $\boldsymbol{\Theta}$ | – control of rotor swash-plates, $\boldsymbol{\Theta} = [\Theta_{01}, \Theta_{02}, \Theta_{11}, \Theta_{12}, \Theta_{21}, \Theta_{22}]^\top$ |

| | |
|------------|--|
| δ_w | – inclination angles of wing flaps (ailerons), $\delta_w = [\delta_{w11}, \delta_{w12}, \delta_{w21}, \delta_{w22}]^\top$ |
| δ_h | – inclination angles of elevators, $\delta_h = [\delta_{h1}, \delta_{h2}, \delta_{h3}]^\top$ |
| δ_v | – inclination angles of rudders, $\delta_v = [\delta_{v1}, \delta_{v2}]^\top$ |
| ω | – angular velocity of rotors, $\omega = [\omega_1, \omega_2]^\top$ |
| τ | – angle of nacelle tilt |

Coefficients

| | |
|---------------------------|--|
| A_r | – characteristic area |
| $C_x(\alpha, \delta)$ | – drag coefficient (in 2D flow) |
| $C_z(\alpha, \delta)$ | – lift coefficient (in 2D flow) |
| $C_{my}(\alpha, \delta)$ | – aerodynamic pitch moment coefficient (in 2D flow) |
| $C_{xc}(\alpha, \delta)$ | – drag coefficient (in 3D flow) |
| $C_{yc}(\alpha, \delta)$ | – side force coefficient (in 3D flow) |
| $C_{zc}(\alpha, \delta)$ | – lift coefficient (in 3D flow) |
| $C_{mxc}(\alpha, \delta)$ | – aerodynamic bank moment coefficient (in 3D flow) |
| $C_{myc}(\alpha, \delta)$ | – aerodynamic pitch moment coefficient (in 3D flow) |
| $C_{mzc}(\alpha, \delta)$ | – aerodynamic yaw moment coefficient (in 3D flow) |
| R_r | – characteristic length |
| V_a | – modulus of motion velocity of section $V_a = \mathbf{V}_a $ |
| $c(y)$ | – chord (characteristic dimension) |
| g | – gravity acceleration |
| m_x | – mass of x -th element |
| α | – angle of attack |
| β | – slip angle |
| δ | – angle of inclination of steering element |
| ρ | – air density |

1. Introduction

In the recent years, increasing interest in tilt rotor technology is observed among rotorcraft community. The development of V-22 aircraft spurred a great research and development effort in tilt rotor aerodynamics (McVeigh *et al.*, 2004), acoustics (Polak and George, 1998), flight control (Weakley *et al.*, 2003), aeroelasticity (Nixon *et al.*, 2003), etc. The next tilt rotor project, Bell-Agusta BA 609, initiated a tilt-rotor design effort in Europe. Recently, several European research projects concerning tilt rotor technology are going on or have already been completed (Cicale, 2003), and some new initiatives appeared. Despite the expanding interest in development and applications of the

tilt-rotor, there are not many papers published in generally accessed literature presenting a comprehensive approach to the tiltrotor modelling and simulation (Polak and George, 1998; McVicar and Bradley, 1992; Srinivas and Chopra, 1996). It was a background for developing at Warsaw University of Technology, a computer model of the tiltrotor for flight simulation and analysis of trim, stability and control in various flight conditions.

2. General model of mobile objects

A tiltrotor computer model was constructed using the generic model of mobile objects, developed at Warsaw University of Technology, to simplify model derivation and simulation of motion for various air, water and land vehicles. This software in the MatLab environment is composed of a main program and sub-programmes performing computations frequently done in dynamics of airplanes, helicopters, sea vessels, etc.

The possibility of the general approach stems from the fact that inertia, gravity and aerodynamic/hydrodynamic loads that act on the vehicles considered are described by the same formulae in reasonably chosen coordinate systems. As a consequence, using this software, computer models of six degrees of freedom motion of various vehicles may be prepared in a fast and efficient way by a proper selection of systems of coordinates and application of supporting subroutines.

Within this software, a vehicle is modelled as the base part ("fuselage") to which other parts/elements of it are joined. These parts may be fixed to the fuselage or may rotate and/or translate relative to it.

Equations of motion are derived in the main system of coordinates fixed to the fuselage by summing loads acting on all elements of the vehicle. These loads are calculated in local coordinate systems fixed to the elements and then transformed to the system of coordinates of the fuselage. It is easy to change the number of elements of a model by adding new or deleting the existing elements and enriching the methods of calculating loads by application of various methods. The computer program for modelling vehicle dynamics is constructed in the same modular way, by applying subroutines for calculating each type of loads and their transformation to the main "fuselage" system of coordinates.

Various subprograms were developed for frequently performed operations like calculation of inertia matrices, flow velocities in different coordinate systems, angles of attack, slip angles, table-look procedures for aerodynamic coefficients, etc.

The generic model was used for the tilt rotor and sea vessel analysis.

3. Tiltrotor model

The tiltrotor model investigated in this study was based on V-22 Osprey aircraft. Due to the modular structure of the software, it is possible to adjust the model to the concepts of tilt-wing, a partly tilting wing or other rotorcraft with different empennage, wings, nacelles, etc.

The tiltrotor (Fig. 1) model is composed of a fuselage, two wings with two trailing edge flaps at each wing, nacelles mounted at the wings tips, rotors mounted in front of the nacelles and a horizontal stabilizer with three flaps and two vertical fins with one rudder mounted on each fin. All components of the aircraft are rigid. The rotors have three blades fixed to the shaft by a pitch bearing. The pitch angles of rotor blades are controlled by swash-plates for constant (collective) and harmonic (cyclic) components.

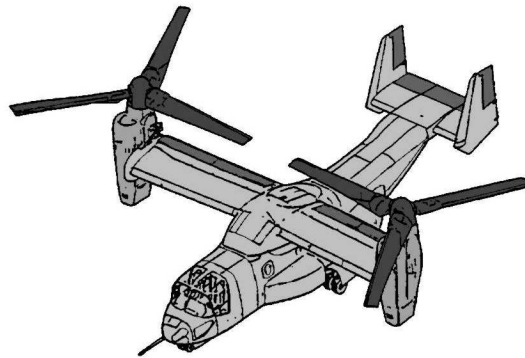


Fig. 1. Configuration of the tiltrotor

The tiltrotor equations of motion are derived in the aircraft coordinate system $O_p x_p y_p z_p$ fixed to the fuselage (Fig. 2). The centre O_p of the aircraft system is placed in the point, where rotor shafts intersect with the fuselage plane of symmetry. The $O_p x_p$ axis lies in the longitudinal symmetry plane of the fuselage, parallel to the horizontal reference plane of the aircraft and is directed "to the cockpit of the aircraft". The $O_p z_p$ axis lies in the longitudinal plane of symmetry of the fuselage and is directed down to the undercarriage. The $O_p y_p$ axis is pointing right, while looking along the $O_p x_p$ axis.

The two other systems of coordinates important for simulation of aircraft motion (Fig. 2) are the *ground coordinate system* $O_g x_g y_g z_g$ fixed to the ground and the *gravity coordinate system* $O_G x_G y_G z_G$ related to the gravity acceleration. The centre of the *ground coordinate system* O_g may be placed in any selected point in space (for instance: a selected point on the airfield). The aircraft motion is simulated from this point. The $O_g z_g$ axis is vertical, it coincides with the direction of the Earth gravity acceleration and is directed

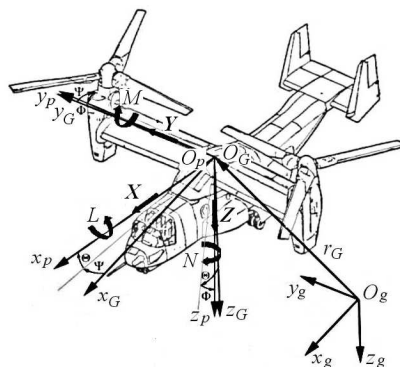


Fig. 2. Systems of coordinates of an aircraft

along its positive value. The axes $O_g x_g$ and $O_g y_g$ lie in the horizontal plane, i.e. the plane perpendicular to the direction of gravity acceleration. The $O_g x_g$ lies along the local geographical meridian pointing north, and the $O_g y_g$ axis points east.

The centre O_G of the gravity *system of coordinates coincides with the centre of fuselage* O_p . The axis of the gravity system is parallel to the axis of the ground coordinate system. The gravity coordinate system is used for describing the position and attitude of the aircraft. The gravity system is translated from the inertia system by the vector $\mathbf{x}_G(t) = [x_G(t), y_G(t), z_G(t)]^\top$, which is a function of time. The vector $\mathbf{x}_G(t)$ describes the translation of the tiltrotor in space. It should be noted here that the point O_G may not be the centre of gravity of the aircraft.

The relation between the gravity and the aircraft system of coordinates is described by Euler's angles of rotation. The relation between the coordinates in both systems is given by an equation

$$\mathbf{x}_p = \mathbf{A}_G(\Psi, \Theta, \Phi) \mathbf{x}_G \quad (3.1)$$

where the rotation matrix \mathbf{A}_G has the form

$$\begin{aligned} \mathbf{A}_G &= \quad (3.2) \\ &= \begin{bmatrix} \cos \Psi \cos \Theta & \sin \Psi \cos \Theta & -\sin \Theta \\ \cos \Psi \sin \Theta \sin \Phi - \sin \Psi \cos \Phi & \sin \Psi \sin \Theta \sin \Phi + \cos \Psi \cos \Phi & \cos \Theta \sin \Phi \\ \cos \Psi \sin \Theta \cos \Phi + \sin \Psi \sin \Phi & \sin \Psi \sin \Theta \cos \Phi - \cos \Psi \sin \Phi & \cos \Theta \cos \Phi \end{bmatrix} \end{aligned}$$

Aircraft motion is described by the vector

$$\mathbf{X} = [\mathbf{V}, \boldsymbol{\Omega}, \mathbf{x}_g, \boldsymbol{\Phi}]^\top = [U, V, W, P, Q, R, x_g, y_g, z_g, \Phi, \Theta, \Psi]^\top \quad (3.3)$$

as a composition of four vectors:

- translation velocity $\mathbf{V} = [U, V, W]^\top$
- rotation (rates) $\boldsymbol{\Omega} = [P, Q, R]^\top$
- Euler's angles written in a vector form $\boldsymbol{\Phi} = [\Phi, \Theta, \Psi]^\top$
- translation of the aircraft relative to the ground $\mathbf{x}_g = [x_g, y_g, z_g]^\top$.

3.1. Equation of motion

Equations of motion of the aircraft are derived using d'Alembert principle, summing up at the point O_p all loads (forces and moments) acting on the fuselage, wings, control surfaces, nacelles, and rotors. The system of six equations of motion is obtained, which may be grouped as two subsystems for forces and moments acting on the fuselage and wings (index p), two nacelles (indices $n1, n2$) and two rotors (indices $r1, r2$)

$$\mathbf{F}_p + \mathbf{F}_{n1} + \mathbf{F}_{n2} + \mathbf{F}_{r1} + \mathbf{F}_{r2} = \mathbf{0} \quad (3.4)$$

$$\mathbf{M}_p + \mathbf{M}_{n1} + \mathbf{M}_{n2} + \mathbf{M}_{r1} + \mathbf{M}_{r2} = \mathbf{0}$$

Each element of the above equations consists of inertia, aerodynamic and gravity parts

$$\mathbf{Q}_{()} = [\mathbf{F}_{()}, \mathbf{M}_{()}]^\top = \mathbf{Q}_{()i} + \mathbf{Q}_{()a} + \mathbf{Q}_{()g} \quad (3.5)$$

3.2. Inertia loads

The expression for inertia loads is obtained from the conservation of momentum, which after performing some mathematical manipulations, may be written in the matrix form

$$\mathbf{Q}_{pb} = \mathbf{I}_p \dot{\mathbf{Y}}_p + \boldsymbol{\Omega}_p \mathbf{I}_p \mathbf{Y}_p \quad (3.6)$$

where the tilt-rotor state vector $\mathbf{Y}_p = [U, V, W, P, Q, R]^\top$ is composed of components of aircraft translation velocity and rates. The inertia matrix has the form

$$\mathbf{I}_p = \begin{bmatrix} m_p & 0 & 0 & 0 & S_{zp} & -S_{yp} \\ 0 & m_p & 0 & -S_{zp} & 0 & S_{xp} \\ 0 & 0 & m_p & S_{yp} & -S_{xp} & 0 \\ 0 & -S_{zp} & S_{yp} & I_{xp} & -I_{xyp} & -I_{xzp} \\ S_{zp} & 0 & -S_{xp} & -I_{xyp} & I_{yp} & -I_{yzp} \\ -S_{yp} & S_{xp} & 0 & -I_{xzp} & -I_{yzp} & I_{zp} \end{bmatrix} \quad (3.7)$$

and the velocity matrix is

$$\mathbf{\Omega}_p = \begin{bmatrix} 0 & -R & Q & 0 & 0 & 0 \\ R & 0 & P & 0 & 0 & 0 \\ -Q & P & 0 & 0 & 0 & 0 \\ 0 & -W & V & 0 & -R & Q \\ W & 0 & -U & R & 0 & P \\ -V & U & 0 & -Q & P & 0 \end{bmatrix} \quad (3.8)$$

Expression (3.6) describes inertia loads acting on the fuselage and on parts of the rotorcraft fixed to it, i.e. wings and control surfaces.

For parts of the aircraft rotating relative to the fuselage, i.e. nacelles (Fig. 3) and rotors, the inertia loads are calculated as

$$\mathbf{Q}_{mb} = \mathbf{I}_m(\dot{\mathbf{Y}}_p + \dot{\mathbf{Y}}_m) + (\mathbf{\Omega}_p + \mathbf{\Omega}_m)\mathbf{I}_m(\mathbf{Y}_p + \mathbf{Y}_m) \quad (3.9)$$

In (3.9), the inertia matrices of rotating elements are calculated in the fuselage system of coordinates.

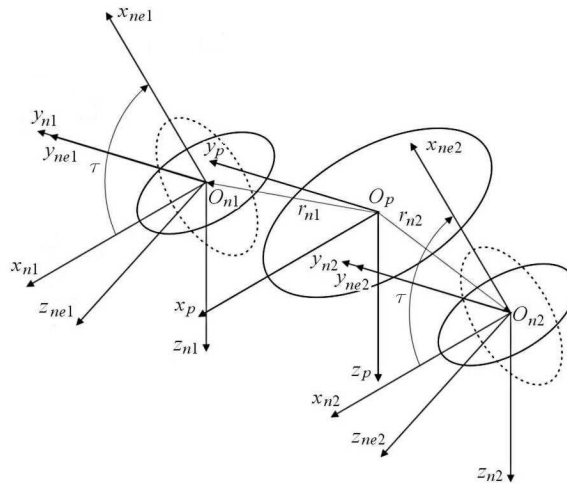


Fig. 3. Nacelle coordinate systems

Additional velocity matrices $\mathbf{\Omega}_m$ are added, containing in a general case the rates and velocities of these elements relative to the fuselage. In the tiltrotor case, they have the form

$$\mathbf{I}_m = \begin{bmatrix} m_m & 0 & 0 & 0 & S_{zm} & -S_{ym} \\ 0 & m_m & 0 & -S_{zm} & 0 & S_{xm} \\ 0 & 0 & m_m & S_{ym} & -S_{xm} & 0 \\ 0 & -S_{zm} & S_{ym} & I_{xm} & -I_{xym} & -I_{xzm} \\ S_{zm} & 0 & -S_{xm} & -I_{xym} & I_{ym} & -I_{yzm} \\ -S_{ym} & S_{xm} & 0 & -I_{xzm} & -I_{yzm} & I_{zm} \end{bmatrix} \quad (3.10)$$

$$\mathbf{\Omega}_m = \begin{bmatrix} 0 & -R_m & Q_m & 0 & 0 & 0 \\ R_m & 0 & -P_m & 0 & 0 & 0 \\ -Q_m & P_m & 0 & 0 & 0 & 0 \\ 0 & 0 & 0 & 0 & -R_m & Q_m \\ 0 & 0 & 0 & R_m & 0 & -P_m \\ 0 & 0 & 0 & -Q_m & P_m & 0 \end{bmatrix}$$

The nonlinear parts of equation (3.9) contain all accelerations acting on the rotating elements, including gyroscopic effects.

3.3. Gravity loads

The gravity forces and moments are calculated first in the centres of gravity of the fuselage and aircraft elements. Next, they are transformed to the centre O_p of the fuselage system of coordinates. The vector of gravity acceleration in the gravity system of coordinates has components

$$\mathbf{g} = [0, 0, g]^T \quad (3.11)$$

It is rotated with respect to the fuselage system of coordinates using the transformation

$$\mathbf{g}_p = \mathbf{A}_G(\Psi, \Theta, \Phi)\mathbf{g} \quad (3.12)$$

The masses of fuselage, wings and empennage are accounted for together and the gravity loads of these parts are calculated as fuselage gravity loads

$$\mathbf{F}_{pg} = m_p \mathbf{g}_p = m_p \mathbf{A}_G \mathbf{g} \quad (3.13)$$

$$\mathbf{M}_{pg} = \mathbf{r}_{CG} \times \mathbf{F}_{pg} = \mathbf{r}_{CG} \times (m_p \mathbf{A}_G \mathbf{g})$$

where the vector \mathbf{r}_{CG} describes the position of C.G. of the fuselage/wings/empennage relative to O_p . The positions of C.G. of other parts of the airplane in the local systems of coordinates are calculated as

$$\mathbf{r}_{CG} = \mathbf{r}_n + \mathbf{A}(\phi, \theta, \psi)\mathbf{r}_{nCG} \quad (3.14)$$

where: \mathbf{r}_n is the vector of C.G. of the given element relative to the fuselage centre, $\mathbf{A}(\phi, \theta, \psi)$ – general description of the matrix of rotation of the local

system of coordinates (fixed to the element) relative to the fuselage system of coordinates (it should be defined separately for each rotating element of the tilt-rotor), \mathbf{r}_{nCG} – vector of the position of CG of the element in the local system of coordinates.

The gravity loads acting on other aircraft elements are transferred to the fuselage system of coordinates by using formulae

$$\mathbf{F}_{ng} = m_n \mathbf{g}_p = m_n \mathbf{A} \mathbf{G} \mathbf{g} \quad (3.15)$$

$$\mathbf{M}_{ng} = [\mathbf{r}_n + \mathbf{A}(\phi, \theta, \psi) \mathbf{r}_{nCG}] \times \mathbf{F}_{ng} = [\mathbf{r}_n + \mathbf{A}(\phi, \theta, \psi) \mathbf{r}_{nCG}] \times [m_n \mathbf{A} \mathbf{G} \mathbf{g}]$$

3.4. Aerodynamics loads

In the generic model, two methods of calculation of quasi-steady aerodynamic loads are used: a 2D model for elongated elements composed of airfoils and a 3D model for solid bodies.

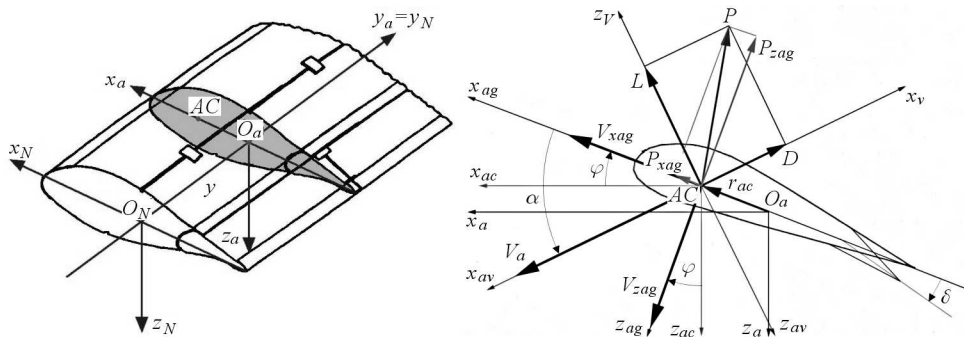


Fig. 4. Two-dimensional flow model

The two dimensional flow (Fig. 4) is used for wings, rotor blades and horizontal and vertical stabilizers. For better description, some coordinate systems are introduced:

- coordinate system of the mounting point of the element $O_N x_N y_N z_N$
- local airfoil coordinate systems $O_a x_a y_a z_a$
- coordinate system fixed to the airfoil aerodynamic centre $O_{ac} x_{ac} y_{ac} z_{ac}$
- coordinate system connected with the geometrically twisted airfoil $O_{ag} x_{ag} y_{ag} z_{ag}$
- coordinate system defined by the vector of velocity of the local airfoil $O_{av} x_{av} y_{av} z_{av}$
- coordinate system of local inflow of the airfoil $O_V x_V y_V z_V$.

The transformation of the mentioned above coordinate systems can be described as

$$\mathbf{x}_N = \mathbf{r}_y + \mathbf{r}_{ac} + \mathbf{A}_{ag}\mathbf{A}_{av}\mathbf{A}_{aV}\mathbf{x}_V = \mathbf{r}_y + \mathbf{r}_{ac} + \mathbf{A}_r\mathbf{x}_V$$

where $\mathbf{A}_r = \mathbf{A}_{ag}\mathbf{A}_{av}\mathbf{A}_{aV}$.

The elongated element is divided along the span for cross sections in which the two dimensional flow is assumed. In each cross section, the instant total flow velocity (Fig. 4) is calculated as

$$\mathbf{V}_{()i} = \mathbf{A}_{r()}\mathbf{A}^{-1}(\mathbf{V} + \boldsymbol{\Omega} \times \mathbf{r}_{()} - \mathbf{A}_G\mathbf{W} + \mathbf{U}_{()} + \Delta\mathbf{W}_{()}) \quad (3.16)$$

taking into account the velocities of:

- a) motion of the fuselage and their aircraft elements in the inertia coordinate system
- b) motion of the air \mathbf{W} due to wind, gusts, etc.
- c) inflow due rotors and wings.

$\mathbf{A}_{r()}$ matrix is a substitute matrix describing rotations of the coordinate systems in airfoil (Fig. 4) from the system of the mounting point of the element to the system of local velocity inflow ($\mathbf{A}_r = \mathbf{A}_{ag}\mathbf{A}_{av}\mathbf{A}_{aV}$). The inflow due rotors and wings $\Delta\mathbf{W}_{()}$ is calculated as

$$\Delta\mathbf{W}_{()} = k_{()}(\mathbf{V} + \boldsymbol{\Omega} \times \mathbf{r}_{()} - \mathbf{A}_G\mathbf{W} + \mathbf{U}_{()}) \quad (3.17)$$

where $k_{()}$ is a coefficient assumed for a given element.

On rotor blades, the rotor induced velocity $\mathbf{U}_{()}$ obtained from Glauert's model is also taken into account while calculating flow velocity. Aerodynamic loads acting in the "aerodynamic centre" (AC) of the cross sections are calculated using aerodynamic coefficients for the airfoil section obtained for the actual airfoil angle of attack α and deflection δ of flaps (if they exist) by a table look procedure. In the cross sections, the vectors of aerodynamic forces and moments are calculated in the flow coordinate system as

$$d\mathbf{P} = [dD, 0, dL]^\top \quad d\mathbf{M} = [0, dM, 0]^\top \quad (3.18)$$

where:

— drag

$$dD = \frac{1}{2}\rho c(y)V_a^2 C_x(\alpha, \delta) dy \quad (3.19)$$

— lift

$$dL = \frac{1}{2}\rho c(y)V_a^2 C_z(\alpha, \delta) dy \quad (3.20)$$

— moment

$$dM = \frac{1}{2}\rho c^2(y)V_a^2 C_{my}(\alpha, \delta) dy \quad (3.21)$$

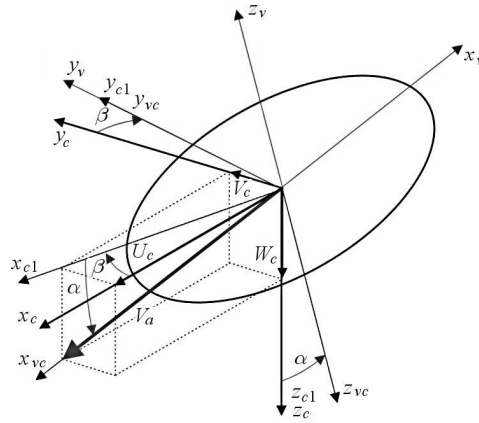


Fig. 5. Three-dimensional airflow

The loads are transferred to the element local system of coordinates, integrated along the span and transferred to the fuselage system of coordinates.

The fuselage and nacelles (Fig. 5) are treated as three-dimensional bodies. Aerodynamic loads, as in the 2D case, are calculated in the centre of local, flow coordinate system

$$P_{()a} = \frac{1}{2} \rho A_r V^2 C_{()c}(\alpha, \beta) \quad (3.22)$$

$$M_{()a} = \frac{1}{2} \rho A_r R_r V^2 C_{m()c}(\alpha, \beta)$$

using the local instant velocity $\mathbf{V}_c = [U_c, V_c, W_c]^T$ in the body aerodynamic centre. The angle of incidence α and angle of slip β are calculated as

$$\alpha = a \sin \frac{W_c}{\sqrt{U_c^2 + V_c^2 + W_c^2}} \quad \beta = a \sin \frac{V_c}{\sqrt{U_c^2 + V_c^2}} \quad (3.23)$$

and the table look procedure is used for obtaining the aerodynamic coefficients. The loads from the flow system of coordinates are transformed to the element system of coordinates using the rotation matrix

$$\mathbf{A}_V = \begin{bmatrix} -\cos \beta \cos \alpha & -\sin \beta & \cos \beta \sin \alpha \\ -\sin \beta \cos \alpha & \cos \beta & \sin \beta \sin \alpha \\ -\sin \alpha & 0 & -\cos \alpha \end{bmatrix} \quad (3.24)$$

Finally, as in the 2D case, the loads are transformed from the element local system of coordinates to the fuselage system of coordinates.

4. Details of modelling tiltrotor parts

4.1. Fuselage

The inertia loads acting on the fuselage are calculated from formula (3.6), gravity loads from (3.13) and the aerodynamic loads from (3.22). The inertia matrix covers the fuselage, wings and empennage – elements fixed to the fuselage.

4.2. Wings

The tiltrotor wings have prescribed planeform, twist and airfoil distribution along the span. At each wing, there are two flaps (ailerons) controlled individually. Flap deflection angles $\boldsymbol{\delta}_w = [\delta_{w11}, \delta_{w12}, \delta_{w21}, \delta_{w22}]^T$ form a part of control variables in the simulation of aircraft motion. The aerodynamic loads are calculated using the 2D model. The induced velocities of rotors are included into velocity of wing airflow calculated in sections along the span.

4.3. Horizontal stabilizer

The horizontal stabilizer forms a part of the empennage and is mounted at the fuselage tail. There are three flaps (elevators) at the trailing edge of the stabiliser, controlled individually. The horizontal stabilizer may have arbitrary airfoil shape and twist angle distribution along the span. The aerodynamic loads are calculated using the 2D model. Influence of the induced velocity of rotors is taken into account in the stabilizer sections along the stabilizer span with the time delay due to the distance travelled from the rotor to empennage. The elevator deflection angles, written as the vector $\boldsymbol{\delta}_h = [\delta_{h1}, \delta_{h2}, \delta_{h3}]^T$ are a part of the vector of control variables.

4.4. Vertical stabilizers

The vertical stabilizers are mounted at the tip of the horizontal stabilizer. There is one flap (rudder) at the trailing edge of each of the two stabilizers, controlled individually. The vertical stabilizers may have arbitrary airfoil shape and twist angle distributions along the span. The aerodynamic loads are calculated using the 2D model. Influence of the induced velocity of the rotors is taken into account in the proper sections along the stabilizer span with the time delay due to the distance travelled from the rotor to empennage. The rudder deflection angles $\boldsymbol{\delta}_v = [\delta_{v1}, \delta_{v2}]^T$ are a part of the vector of control variables.

4.5. Engine nacelles

The engine nacelles are placed at the tip of each wing. They may rotate about the axis perpendicular to the fuselage plane of symmetry. The nacelles inertia loads are calculated using expression (3.10) and gravity loads using expression (3.15). Aerodynamic loads are calculated using the 3D model. The velocity of airflow around the nacelles contains inflow from the rotors and a component due to rotation of nacelles about the fuselage axis. The angle of nacelle rotation τ is included into the set of control variables.

4.6. Rotors

The rotors rotation axes are perpendicular to the axis of nacelle rotation relative to the fuselage. When the rotor axes are in the horizontal position, the right rotor rotates clockwise, and the left counter-clockwise looking from the rear of the fuselage. For calculations of inertia loads, the rotors are treated as rotating discs and in the hub system of coordinates, the inertia matrices have the form

$$\mathbf{I}_{ri} = \begin{bmatrix} m_{ri} & 0 & 0 & 0 & 0 & 0 \\ 0 & m_{ri} & 0 & 0 & 0 & 0 \\ 0 & 0 & m_{ri} & 0 & 0 & 0 \\ 0 & 0 & 0 & 0 & 0 & 0 \\ 0 & 0 & 0 & 0 & 0 & 0 \\ 0 & 0 & 0 & 0 & 0 & I_{zri} \end{bmatrix} \quad (4.1)$$

The final form of inertia matrices of rotors (3.10)₁ results from nacelle and rotors rotation about the fuselage axis.

Each rotor has three blades mounted to the shaft by pitch bearings. The pitch of the rotor blades is controlled by the swash-plate, resulting in collective and periodic control in the form

$$\theta_{ij} = \theta_{0i} + \theta_{1i} \cos\left(\Omega_i t + \frac{2\pi}{3} j\right) + \theta_{2i} \sin\left(\Omega_i t + \frac{2\pi}{3} j\right) \quad (4.2)$$

The blades may have arbitrary planeform, twist and airfoil distribution along the span. The aerodynamic loads are calculated using strip theory with quasisteady aerodynamic loads using the table-look procedure for calculations of aerodynamic coefficient of airfoils (2D model described above). The induced flow is calculated using Glauert's model. The control of rotor swash-plates may be written in the vector form $\Theta = [\theta_{01}, \theta_{02}, \theta_{11}, \theta_{12}, \theta_{21}, \theta_{22}]^T$ containing the sub-set of tiltrotor control variables.

The control vector of the tiltrotor

$$\mathbf{C} = [\tau, \delta_w, \delta_h, \delta_v, \Theta]^T \quad (4.3)$$

consists of (respectively) tilt angle of nacelles, angles of deflection of ailerons, elevators and rudders, pitch control of rotors, which is 16 control states. The angular velocity of the rotor is assumed constant.

5. Calculation of trim in steady flight

Including inertia loads into the general form of equations of motion, the tiltrotor equations of motion have the form

$$\begin{aligned} \mathbf{l}_p \dot{\mathbf{Y}}_p + \boldsymbol{\Omega}_p \mathbf{l}_p \mathbf{Y}_p + \sum_{i=1}^2 (\mathbf{l}_{ni} \dot{\mathbf{Y}}_{ni} + \boldsymbol{\Omega}_{ni} \mathbf{l}_{ni} \mathbf{Y}_{ni}) + \sum_{i=1}^2 (\mathbf{l}_{ri} \dot{\mathbf{Y}}_{ri} + \boldsymbol{\Omega}_{ri} \mathbf{l}_{ri} \mathbf{Y}_{ri}) = \\ = \mathbf{Q}_{pg} + \sum_{i=1}^2 \mathbf{Q}_{nig} + \sum_{i=1}^2 \mathbf{Q}_{rig} + \mathbf{Q}_{pa} + \sum_{i=1}^2 \mathbf{Q}_{nia} + \sum_{i=1}^2 \mathbf{Q}_{ria} \end{aligned} \quad (5.1)$$

In a steady flight, the accelerations are zero and the equations of motion are reduced to a system of 6 algebraic equations

$$\begin{aligned} \mathbf{Q} = -\boldsymbol{\Omega}_p \mathbf{l}_p \mathbf{Y}_p - \sum_{i=1}^2 (\mathbf{l}_{ni} \dot{\mathbf{Y}}_{ni} + \boldsymbol{\Omega}_{ni} \mathbf{l}_{ni} \mathbf{Y}_{ni}) - \sum_{i=1}^2 (\mathbf{l}_{ri} \dot{\mathbf{Y}}_{ri} + \boldsymbol{\Omega}_{ri} \mathbf{l}_{ri} \mathbf{Y}_{ri}) + \\ + \mathbf{Q}_{pg} + \sum_{i=1}^2 \mathbf{Q}_{nig} + \sum_{i=1}^2 \mathbf{Q}_{rig} + \mathbf{Q}_{pa} + \sum_{i=1}^2 \mathbf{Q}_{nia} + \sum_{i=1}^2 \mathbf{Q}_{ria} = \mathbf{0} \end{aligned} \quad (5.2)$$

For trim conditions the equations of motion have the general form

$$\mathbf{Q}(\mathbf{V}_p, \boldsymbol{\Omega}_p, \boldsymbol{\Phi}, \tau, \boldsymbol{\delta}_w, \boldsymbol{\delta}_h, \boldsymbol{\delta}_v, \boldsymbol{\Theta}) = \mathbf{0} \quad (5.3)$$

The values of trim controls in a steady flight are calculated using the Levenberg-Marquardt method to minimise total loads (5.3) acting on the tiltrotor. This approach (Miller, 2004) allows one to obtain the trim states for the cases when the number of calculated trim parameters is arbitrary, i.e. less, equal or greater than the number of equations of motion.

Minimizing the nonlinear functions numerically leads to computation of local minima, which may not be the real solution of the trim from the physical point of view. To avoid such cases, the total loads acting on the tiltrotor in a steady flight were monitored. Simulations of the tiltrotor flight were done using controls calculated in the trim procedure to prove that the parameters obtained by the minimisation method were correct.

5.1. Data for simulation

The aim of simulation performed in this study was to check the validity of the model and to get insight into tiltrotor behaviour in the trimmed state. Data of V-22 were used in the simulation. A part of the design data was taken from accessible literature (e.g., Miller and Narkiewicz, 2003; [11]). For parameters with no available data, the values were assumed as for corresponding parts of a similar aircraft (Miller, 2004). Base dimensions of the simulated tiltrotor are shown in Fig. 6 (Miller and Narkiewicz, 2003) and given in Table 1.

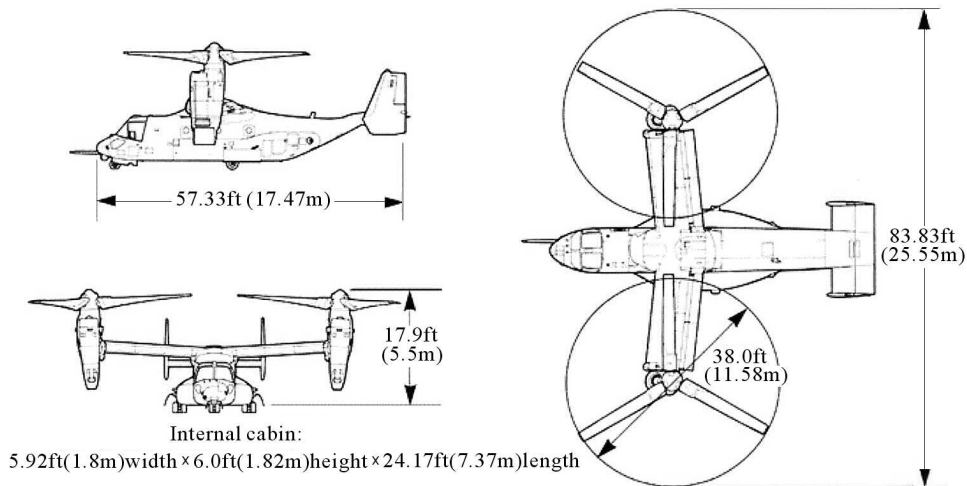


Fig. 6. Dimensions of V-22

Table 1. Tiltrotor data

| Rotor System | | |
|---------------------------------|-----------------------------------|-------------------|
| Number of blades | | 3 |
| Blades tip speed | m/s (fps) | 201.75 (661.90) |
| Diameter | m (ft) | 11.58 (38.00) |
| Disc area | m ² (ft ²) | 210.70 (2 268.00) |
| Weights | | |
| Take off | kg (lbs) | 15 032 (33 140) |
| Dimensions | | |
| Length, fuselage | m (ft) | 1 748 (57.33) |
| Width, rotors turning | m (ft) | 25.55 (83.33) |
| Width, horizontal stabilizer | m (ft) | 5.61 (18.42) |
| Height, nacelles fully vertical | m (ft) | 6.63 (21.76) |
| Height, vertical stabilizer | m (ft) | 5.38 (17.65) |

5.2. Results of simulations

Before simulating motion of the complete tiltrotor, separate modules and complete codes were debugged. Next, for the tiltrotor data, the results of simplified cases were checked for consistency with the proper reactions on the input. For instance, analysis of the influence of each control surfaces (Miller, 2004; Miller and Narkiewicz, 2001) on the tiltrotor flight was done for the selected flight phases (Swertfager and Martin, 1992). The tiltrotor flight simulations were done for three tiltrotor flight modes: helicopter, airplane and conversion.

The longitudinal, symmetrical cases of the flight are presented in this paper. The side velocity V , angular velocities P , Q , R roll Φ and yaw Ψ angles as well as the rudder deflection angles $\delta_v = \delta_{v1} = \delta_{v2}$ were assumed zero. The same values were assumed for the deflection of wing flaps $\delta_w = \delta_{w11} = \delta_{w12} = \delta_{w21} = \delta_{w22}$, angles of elevators $\delta_h = \delta_{h1} = \delta_{h2} = \delta_{h3}$ and collective control of the rotor pitch $\Theta_0 = \Theta_{01} = \Theta_{02}$ for flaps on the wings and elevator. The longitudinal cyclic control of the rotor was assumed symmetrical and $\Theta_1 = \Theta_{11} = \Theta_{12}$, whereas the lateral cyclic control unsymmetrical $\Theta_2 = \Theta_{21} = -\Theta$.

During the trim calculations for the assumed values of forward U and vertical W flight velocities, the tiltrotor pitch angle Θ , deflection of flaps on the wing δ_w and elevators δ_h , collective Θ_0 and cyclic Θ_1 pitch of rotor blades and the nacelle tilt angle τ were computed.

The airplane, conversion and helicopter modes of the tiltrotor flight were considered.

The results of a steady flight in the airplane mode (horizontal with vertical climb) are given in Fig. 7-Fig. 10. The forward flight velocity was changed within the range $U = 10$ -180 m/s, and the vertical velocity was changed within the range $W = -20$ -20 m/s.

The tiltrotor pitch angle obtained from simulations was equal 0 for the assumed flight conditions, and it was not presented in graphs. The calculated deflection angles of wing flaps (Fig. 7) and elevators (Fig. 8) did not exceed the values of available control surface deflections of V-22.

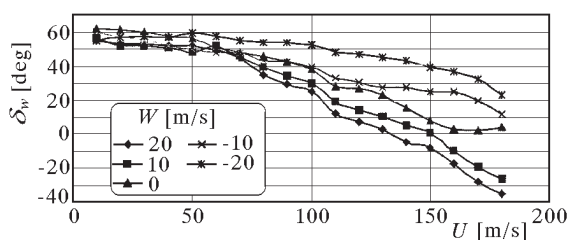


Fig. 7. Deflection of flaps

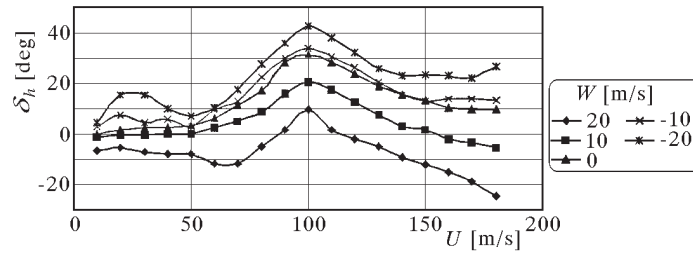


Fig. 8. Deflection of elevators

The collective control of the rotor (Fig. 9) is almost proportional to forward speed. When the forward speed is low (below 60 m/s), the minimal tilt angle of nacelles (Fig. 10) assuring proper values of the lift is about 70° . The deflection of wing flaps is maximum for low forward speed, to balance the inclination of lift from the rotors. The deflection of elevators is maximum, when the aircraft is in the conversion mode because of the necessity to provide a proper tiltrotor pitch moment. It has the maximum value when the conversion stops and the rotor axis is in the horizontal position.

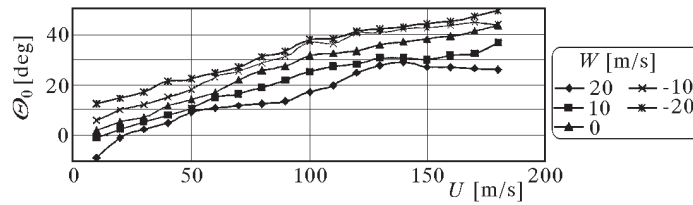


Fig. 9. Collective pitch

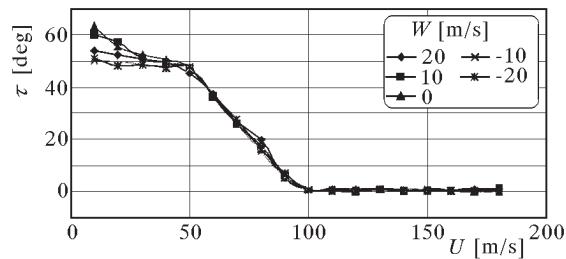


Fig. 10. Tilt angle of nacelles

5.3. Steady forward flight with vertical climb in conversion mode

In the conversion mode, a steady forward flight with vertical climb velocity with possible deflection angle of the nacelle was simulated. The forward flight velocity was changed within the range $U = 20\text{-}180$ m/s.

As in the previous case, the values of calculated deflection angles of wing flaps (Fig. 11) and elevators (Fig. 12) do not exceed the values of available control for V-22. The collective pitch of rotor is approximately proportional to forward speed. The deflection of wing flaps (Fig. 11) is maximum for low forward speed. When the forward speed is low, the minimum tilt angle of nacelles (Fig. 14) is about 55° assuring the proper aerodynamic lift. It becomes smaller (about 43°) when the forward speed increases.

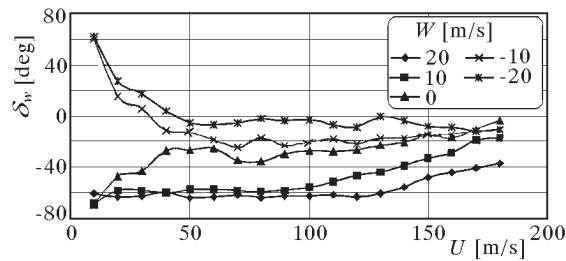


Fig. 11. Deflection of flaps

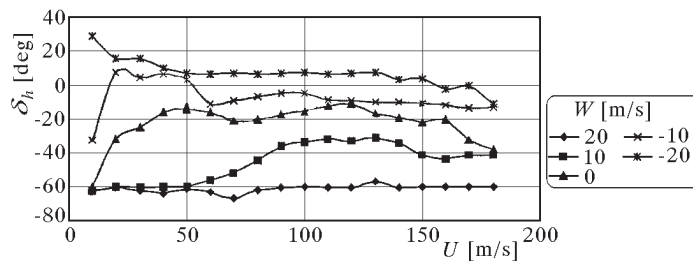


Fig. 12. Deflection of elevators

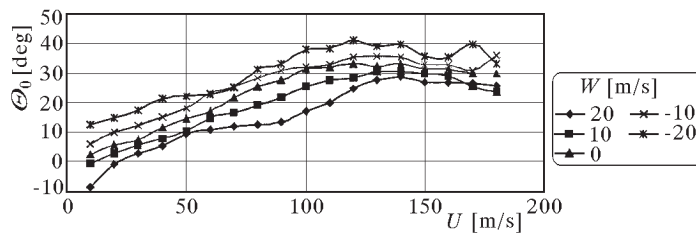


Fig. 13. Collective pitch

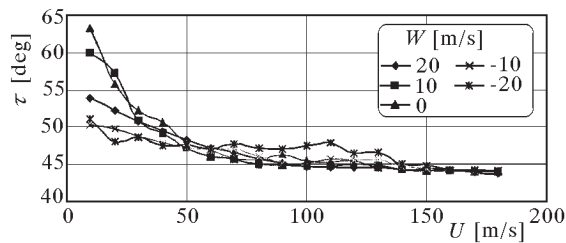


Fig. 14. Tilt angle of nacelles

5.4. Steady forward flight with vertical climb in helicopter mode

In the helicopter mode, a steady forward flight with vertical climb with the tilt angle of the nacelles 90° was simulated. The forward flight velocity was changed within the range $U = -70-70$ m/s. The vertical velocity was changed within the range $W = -20-20$ m/s.

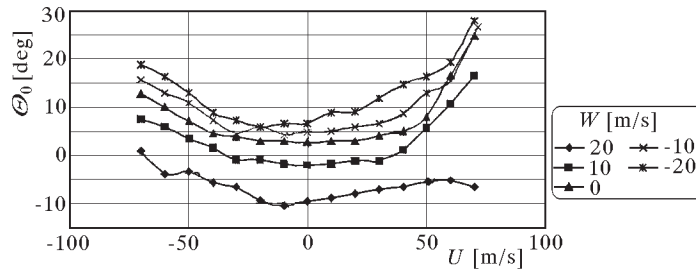


Fig. 15. Collective pitch

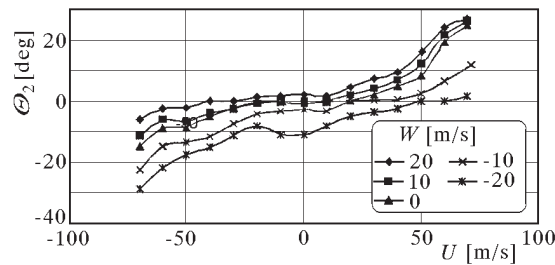


Fig. 16. Cyclic control (longitudinal)

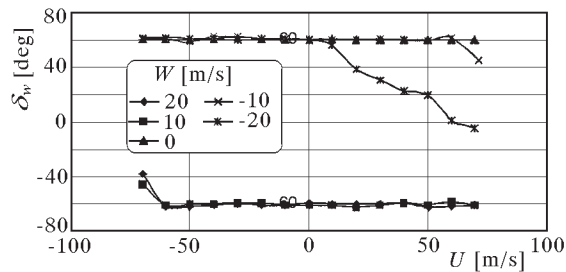


Fig. 17. Deflection of flaps

For the assumed steady flight conditions, the negligible small value of pitch angle of the tiltrotor is obtained. The collective control of rotor swash-plates (Fig. 15) increases with the increase of vertical speed. The cyclic control of rotor pitch (Fig. 16) varies in the opposite way: when the vertical speed increases, the pitch angle of tiltrotor is also stabilized. The inclination angles

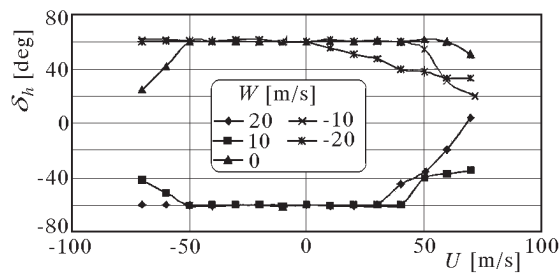


Fig. 18. Deflection of elevators

of wing flaps (Fig. 17) and elevators (Fig. 18) obtained in calculations do not exceed available values for V-22. In the range of negative forward speed, the influence of flap deflection on tiltrotor motion is not substantial, but it becomes noticeable at positive forward speed greater than 10-20 m/s. The sign of deflection of control surfaces depends on the direction of vertical speed.

5.5. Side flight in helicopter mode

In the side flight in the helicopter mode, the forward flight velocity was changed within the range $U = -70-70$ m/s, and the side flight velocity was changed within the range $V = -20-20$ m/s. The tiltrotor vertical velocity the $W = 0$. The lateral cyclic pitch control was symmetrical $\Theta_1 = \Theta_{11} = \Theta_{12}$ and longitudinal cyclic control – unsymmetrical $\Theta_2 = \Theta_{21} = -\Theta_{22}$. The aircraft pitch and yaw angles, pitch and yaw rates and both rudder deflections were assumed zero.

From equilibrium conditions, the roll angle of tiltrotor Φ , inclination angles of wing flaps $\delta_w = \delta_{w11} = \delta_{w12} = \delta_{w21} = \delta_{w22}$, inclination angles of elevators $\delta_h = \delta_{h1} = \delta_{h2} = \delta_{h3}$ and collective control of the rotor swash-plate $\Theta_0 = \Theta_{01} = \Theta_{02}$ were calculated. The results are shown in Fig. 19 - Fig. 24.

In these flight conditions, the tiltrotor roll angle depends on side velocity. The deflections of flaps and elevators are small. The value of the cyclic pitch control depends on the value of side speed and its sign.

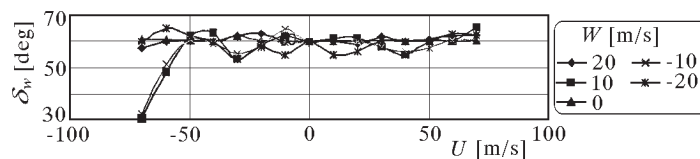


Fig. 19. Deflection of flaps

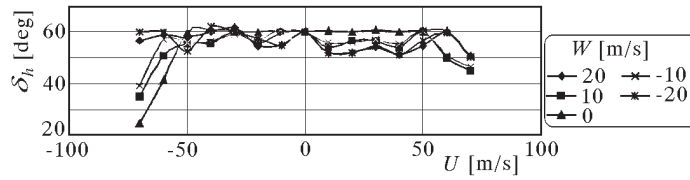


Fig. 20. Deflection of elevators

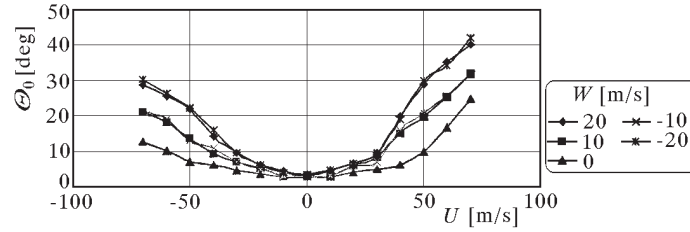


Fig. 21. Collective pitch

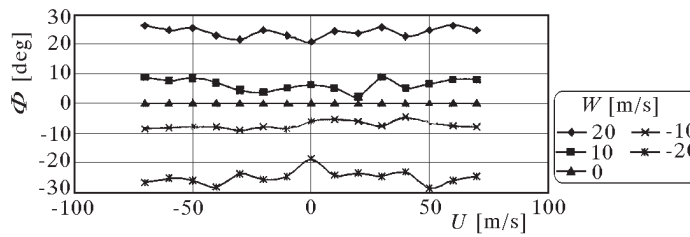


Fig. 22. Roll angle of tiltrotor

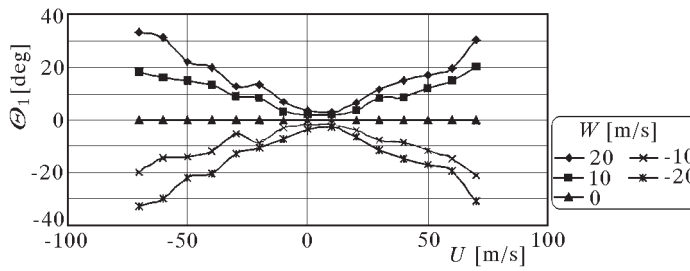


Fig. 23. Cyclic control (lateral)

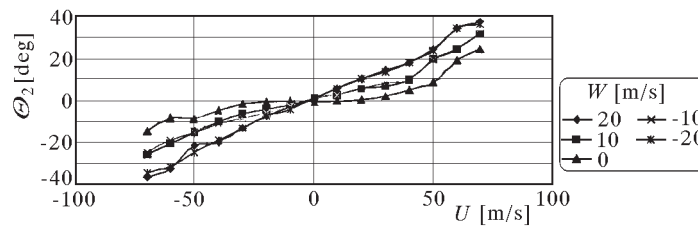


Fig. 24. Cyclic control (longitudinal)

5.6. Stability and controllability

For stability analysis, of the tiltrotor the equations of motion are numerically linearized with respect to state and control variables for given trim values. This allows analysis of the control matrix and calculation of eigenvalues and eigenvectors for examination stability. This option of model analysis allows one to investigate the stability and controllability of the aircraft.

For the assumed tiltrotor design data, both stability and controllability analysis was made for the whole forward speed range of the tiltrotor. In the range of velocity considered, complex eigenvalues with negative real parts were obtained only for low velocity of forward flight (from 60 to 70 m/s), when the conversion mode occurs. In other forward speed, negative real parts of eigenvalues were obtained. These results show that in the steady flight, the aircraft is stable in the whole range of flight velocities.

Analysing the control matrix, it may be stated that the control variables influence the related loads with minor cross-coupling effects. For the airplane mode, this is summarized in Table 2.

Table 2. Controllability analysis in the airplane mode

| Loads | Control elements | | |
|-------|---|---|---|
| | airplane mode | transition | helicopter mode |
| F_x | rotor collective pitch | nacelles tilt angle, rotor collective pitch | rotor longitudinal cyclic pitch |
| F_y | rudders (no lateral cyclic pitch) | rudders (no lateral cyclic pitch) | rotor lateral cyclic pitch |
| F_z | flaps, elevators (not nacelles tilt nor longitudinal cyclic pitch used) | flaps, nacelles tilt, rotor collective pitch, elevators (smaller influence) | rotor collective pitch |
| M_x | flaps, elevators, rotor collective pitch | deflection of flaps, rotor collective control | asymmetric rotor collective pitch |
| M_y | elevators (rotor longitudinal cyclic pitch not used) | deflection of elevators, rotor collective control | rotor longitudinal cyclic pitch (symmetric) |
| M_z | rotor collective pitch, rudders | rotor collective pitch, rudders | rotor collective pitch, rotor longitudinal cyclic pitch |

5.7. Results of numerical simulations

For the calculated steady flight parameters, simulations of flight were carried out to check their accuracy. The steady flight in the airplane mode was simulated for: $U = 180 \text{ m/s}$, $V = W = P = Q = R = 0$, $\Phi = \Theta = \Psi = 0$ and the trim parameters obtained from calculations were: deflection of wing flaps $\delta_w = -6.75^\circ$, elevators $\delta_h = 7.23^\circ$ and collective pitch of the rotor $\Theta_0 = 45.91^\circ$.

The tiltrotor displacements are presented in Fig. 25 (horizontal) and in Fig. 26 (vertical). The variations of attitude angles are very small (below 0.1°).

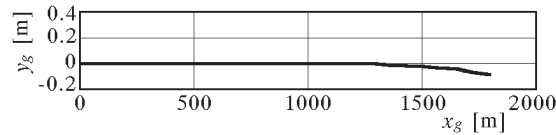


Fig. 25. Horizontal displacement in the airplane mode

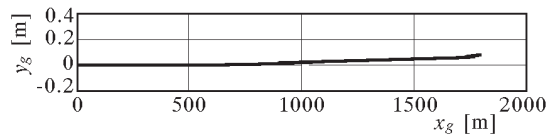


Fig. 26. Vertical displacement in the airplane mode

It can be seen that during 1800 m distance, the flight altitude decreased by about 0.1 m and side translation was about 0.1 m to the left. These values are attributed to numerical errors in calculation of the trim values. Similar results were obtained in the transition and helicopter modes.

6. Conclusions

The tiltrotor computer model was developed for flight simulation, trim stability and control analysis. The model is composed of rigid elements: fuselage, wings, empennage, rotors, but due to the modularity of the code these assumptions may be easily released. The design parameters of V-22 tiltrotor were used for simulations. Some data of the tiltrotor had to be assumed, and there was no possibility to compare the results of numerical simulations with the flight data. On the grounds of results of calculations performed, it may be concluded that the developed model of the tiltrotor works properly.

A tiltrotor is a complex rotorcraft, and several simplifying assumptions had to be applied. They might be released by adjusting the model for specific needs of a particular helicopter.

Acknowledgement

The research was carried out as a part of a project supported by the State Committee for Scientific Research "The research on the control of tiltrotor in selected flight stages", grant No. 5 T12C 067 24.

References

1. CICALÉ M., 2003, ERICA: the European tiltrotor design and critical technology projects, *29th European Rotorcraft Forum*, Friedrichshafen, Germany
2. MCVEIGH M.A., NAGIB H., WOOD T., KIEDAISCH J., STALKER A., WYGNANSKI I., 2004, Model and full scale tiltrotor download reduction tests using active flow control, *60th Annual Forum*, **1**, Baltimore, MD
3. McVICAR J.S.G., BRADLEY R., 1992, A generic tilt-rotor simulation model with parallel implementation and partial periodic trim algorithm, *18th European Rotorcraft Forum*, Avignon, France
4. MILLER M., 2004, *The Control of Tiltrotor in Chosen Flight Stages*, Ph.D. Thesis, Warsaw, Poland
5. MILLER M., NARKIEWICZ J., 2001, Control of tiltrotor aircraft, *4th National Rotorcraft Forum*, Warsaw, Poland
6. MILLER M., NARKIEWICZ J., 2003, Simulation of tiltrotor motion, *29th European Rotorcraft Forum*, Friedrichshafen, Germany
7. NIXON M.W. ET AL., 2003, Aeroelastic stability of a four-bladed semi-articulated soft-in-plane tiltrotor model, *59 AHS Forum*, **110**, Phoenix, AZ, USA
8. POLAK D.R., GEORGE A.R., 1998, Flowfield and acoustic measurements from a model tiltrotor in hover, *Journal of Aircraft*, **35**, 6, 921-929
9. SRINIVAS V., CHOPRA I., 1996, Validation of a comprehensive aeroelastic analysis for tiltrotor aircraft, *AHS 52nd Annual Forum*, Washington, D.C., USA
10. SWERTFAGER T.A., MARTIN S. JR., 1992, The V-22 for SOF, *48th American Helicopter Society Annual Forum*, Washington, D.C.
11. *V-22 Osprey Technical Specifications*, <http://www.boeing.com/rotorcraft/military/v22/v22spec.htm>
12. WEAKLEY J.M., KLEINHESSELINK K.M., MASON D.H., MITCHELL D.G., 2003, Simulation evaluation of V-22 degraded-mode flying qualities, *59 AHS Forum*, **135**, Phoenix, AZ, USA

Modelowanie tiltrotora dla symulacji w różnych stanach lotu

Streszczenie

Opracowano symulacyjny model statku powietrznego typu tiltrotor przeznaczony do symulacji lotu oraz analizy osiągow, stabilności i sterowania. Model wiroplata złożony jest z kadłuba, skrzydeł, usterzenia ogonowego, gondoli silnikowych i wirników. Równania ruchu zostały uzyskane przez sumowanie obciążeń od sił bezwładności, grawitacyjnych i aerodynamicznych działających na każdy element statku powietrznego. Obciążenia aerodynamiczne skrzydeł, stateczników i łopat wirników zostały obliczone z zastosowaniem quasistacjonarnego modelu opływu. Do wyznaczania prędkości indukowanej wirników zastosowano model Glauerta. Wpływ strumienia zawirnikowego na skrzydła i stateczniki jest obliczany z wykorzystaniem aktualnej wartości prędkości indukowanej wirników. Program do modelowania wiroplata został opracowany w środowisku MatLab. Program zbudowany jest z modułów obliczeń obciążeń poszczególnych elementów wiroplata, które wykorzystywane są również do wyznaczania warunków lotu ustalonego, stateczności i sterowności. Podczas pierwszego etapu badań wyznaczono warunki ustalonego lotu tiltrotora w różnych konfiguracjach, co pozwoliło zbadać zachowanie i potwierdzić poprawność modelu.

Manuscript received February 9, 2006; accepted for print July 5, 2006